STRUCTURAL CONTROL AND HEALTH MONITORING
Struct. Control Health Monit. (2016)
Published online in Wiley Online Library (wileyonlinelibrary.com). DOI: 10.1002/stc.1906

Shake table investigation of a structure isolated by recycled rubber devices and magnetorheological dampers

Giuseppe Maddaloni[1,3,*,†], Nicola Caterino[2,3] and Antonio Occhiuzzi[2,3]

[1]*Department of Engineering, University of Benevento 'Sannio', Benevento 82100, Italy*
[2]*Department of Engineering, University of Naples 'Parthenope', Naples 80143, Italy*
[3]*Construction Technologies Institute, Italian National Research Council (ITC-CNR), San Giuliano Milanese (MI), Italy*

SUMMARY

This paper describes the main results obtained from shaking table tests performed on a 1-storey steel frame isolated by innovative rubber bearings and magnetorheological dampers (hybrid isolation). The proposed base isolation technology is based on the use of bearings made of a low-cost recycled elastomer and reinforced with fibre sheets. Bounding the strain demand for such isolators because of severe earthquakes within acceptable values is a key point of this research, crucial for the effective application of this low-cost technology to real cases. A specific semi-active controller has been designed and adopted to achieve this goal. A set of natural earthquake records is applied to the base of the said structure using a shaking table system. The experimental results in terms of base displacement, roof acceleration and interstory drift are compared with the response of the same structure base isolated in the absence of magnetorheological dampers. It is found that when the semi-active control is suitably designed and implemented, the seismic performance of the structure can be significantly improved. Even if referred to the case study, the conclusions encourage further investigating the application of the proposed low-cost technology for seismic protection of buildings. © 2016 The Authors. Structural Control and Health Monitoring Published by John Wiley & Sons, Ltd.

Received 31 March 2015; Revised 6 April 2016; Accepted 30 May 2016

KEY WORDS: base isolation; low-cost rubber isolator; semi-active control; shaking table test; magnetorheological damper

1. INTRODUCTION

Seismic base isolation (BI) is one of the most successful techniques used to protect structures against earthquakes. Many different devices can be adopted to implement such control strategy [1]. However, observations from recent earthquakes have demonstrated that an isolation system alone in some cases cannot provide a full protection against structural damage given that a base-isolated building may experience large and unexpected displacements, especially because of near-field earthquakes [2]. Such excessive displacements are generally undesirable for many reasons, not least the possible collision with adjacent constructions [3].

In recent years, several researchers have investigated the possibility of using supplemental dampers to reduce displacement demand for base-isolated structures. This is the concept of the hybrid BI system. In a BI system, the use of passive dampers as supplemental devices is not always agreed upon. Actually, in such cases, the base displacement demand is generally reduced, even if interstory drifts and floor accelerations may increase [4]. The use of adaptive 'smart' dampers is proposed herein to enhance the performance of a BI system, avoiding the above undesired.

*Correspondence to: Giuseppe Maddaloni, Department of Engineering, University of Benevento 'Sannio', Palazzo ex-INPS - Piazza Roma, 21, 82100 Benevento, Italy.
†E-mail: giuseppe.maddaloni@unisannio.it

A pioneering study on hybrid isolation through the use of variable dampers was proposed by Makris in 1997 [5]. In particular, in this paper, the problem of protecting base-isolated structures from rapid, long-period motions is addressed. He shows that in certain cases, the presence of high-friction forces in the isolation system of a structure is responsible for the presence of permanent displacements. Electrorheological dampers can eliminate this problem because the friction forces can be removed during shaking, thus allowing the superstructure to be recentred once the seismic action is ended. Subsequently, a design approach for the use of semi-active (SA) devices in base-isolated buildings was proposed by Li and Ou [6]. The effectiveness of the SA control of base-isolated structures was tested in several experiments. In Madden *et al.* [7], the ability of an adaptive seismic isolation system to protect structures subjected to earthquake ground motions was investigated. The isolation system consists of sliding isolation bearings in combination with an adaptive hydraulic damper. The damping capacity of the hydraulic damper can be modified in real time to respond to the effects that the earthquake ground motion has on the structure. An experimental laboratory implementation of the adaptive isolation system within a scale-model building structure was described. The experimental results demonstrated that for both near-field and far-field earthquake ground motions, an adaptive sliding BI system is capable of reducing the interstory drift response of structures while simultaneously limiting the displacement response of the isolation system.

Other experimental studies have been conducted on hybrid BI systems by pairing rubber bearings with magnetorheological (MR) dampers [8,9]. In particular, in [8], a series of large-scale experimental tests was conducted on a mass equipped with a BI system that consists of high-damping rubber bearings and an MR damper. The specimen was subjected to various intensities of near- and far-fault earthquakes. The results showed that high-damping rubber bearings can reduce the absolute acceleration of the mass but that they also allow large displacements. Therefore, an MR damper is needed to control displacement. In [9], the performance of an isolation system for a base-isolated, two-degree-of-freedom structural model employing MR fluid dampers was investigated. The efficacy of this smart system in reducing structural responses for a wide range of loading conditions was demonstrated in a series of experiments. The results for the smart solution were compared with tests wherein an MR damper was operated in a passive mode (i.e. with a constant current being applied to the MR damper). A comparison between numerical and experimental results obtained using isolated structures controlled with MR dampers is shown in [10] and [11].

Researchers' efforts on hybrid isolation systems realised using MR dampers have been focused on the development of new control algorithms for reducing the response of base-isolated structures [12–14]. In [14], two control algorithms were developed to monitor the voltage input to an MR damper so that the desirable performance of the structural system could be achieved. The novelty of the models is that they consider, for the first time, the effect of the supplied voltage on the commanded voltage dynamics of the MR damper. The efficiency of the proposed techniques has been shown and compared using an example of a base-isolated three-storey building subject to a set of seismic excitations. An interesting hybrid BI system composed of linear elastomeric bearings, friction-pendulum bearings, shape-memory alloy wires and magnetorheological dampers was proposed for the mitigation of seismic motions by Shook *et al.* [15].

To compare different isolation systems, such as rubber bearings, friction pendulums and roller systems, a wide experimental campaign was recently conducted in Naples (Italy) under the framework of the Joint Experimental Testing on Base Isolation Systems (JETBIS) program, which is financed by the Italian Department of Civil Protection. In particular, the seismic performance of a steel frame that is isolated with an innovative type of rubber bearing was evaluated by shaking table tests. The novel BI technology consists of bearings made of a low-cost recycled elastomer and reinforced with fibre sheets [16]. For sites requiring large design displacements (e.g. in some epicentral areas), the rubber bearings cannot be used in the absence of dampers that are used in parallel. Therefore, the behaviour of the same base-isolated structure described earlier, but also equipped with MR dampers (hybrid isolation), is experimentally investigated using the shaking table. The present paper describes the main results obtained comparing the seismic response of the base-isolated structure with that of the same structure equipped with the hybrid control system.

DOI: 10.1002/stc

2. DESCRIPTION OF EXPERIMENTAL TESTS

In the following, the main features of the JETBIS structural mock up (test setup and instrumentation) are introduced.

2.1. Test setup configuration

The shake table tests, which are performed to investigate the seismic behaviour of the hybrid BI system, were conducted at the laboratory of the Department of Structures for Engineering and Architecture of the University of Naples Federico II. The tests were performed using an earthquake simulator system, which consists of two 3 × 3 m square shake tables. Each table is characterised by two degrees of freedom in the two horizontal directions. The maximum payload of each shake table is 200 kN with a frequency range of 0–50 Hz, peak acceleration equal to 1 g at the maximum payload, peak velocity equal to 1 m/s and total displacement equal to 500 mm (±250 mm). Only one shake table was used in this experimental campaign.

The test setup is shown in Figure 1(a) and (b). It was adapted from one previously used for experimental tests at the same laboratory [17,18]. The test frame has a height of 2900 mm and plan dimensions of 2150 × 2650 mm. The frame is constructed using welded square hollow columns (150 × 150 × 15 mm) of C45 steel material and rolled square hollow beams (120 × 120 × 12.5 mm) of S275 steel material; the beam–column connections are bolted. A 3.3-tons reinforced concrete slab is placed on the roof of the structure. Its plan dimensions are 2150 × 2650 mm with a thickness equal to 250 mm. The concrete slab is connected to the test frame by prestressed bolts to guarantee sufficient friction strength at the steel-beam-to-slab interface for the transfer of inertia forces.

A total mass of 3.6 tons is added at the base of the frame using concrete blocks. The mass is restrained on the shaking table by a rigid horizontal frame (in red) fixed at the vertical frame, as shown in Figure 1(b). The total mass of the setup (vertical steel frame + top concrete slab + concrete blocks

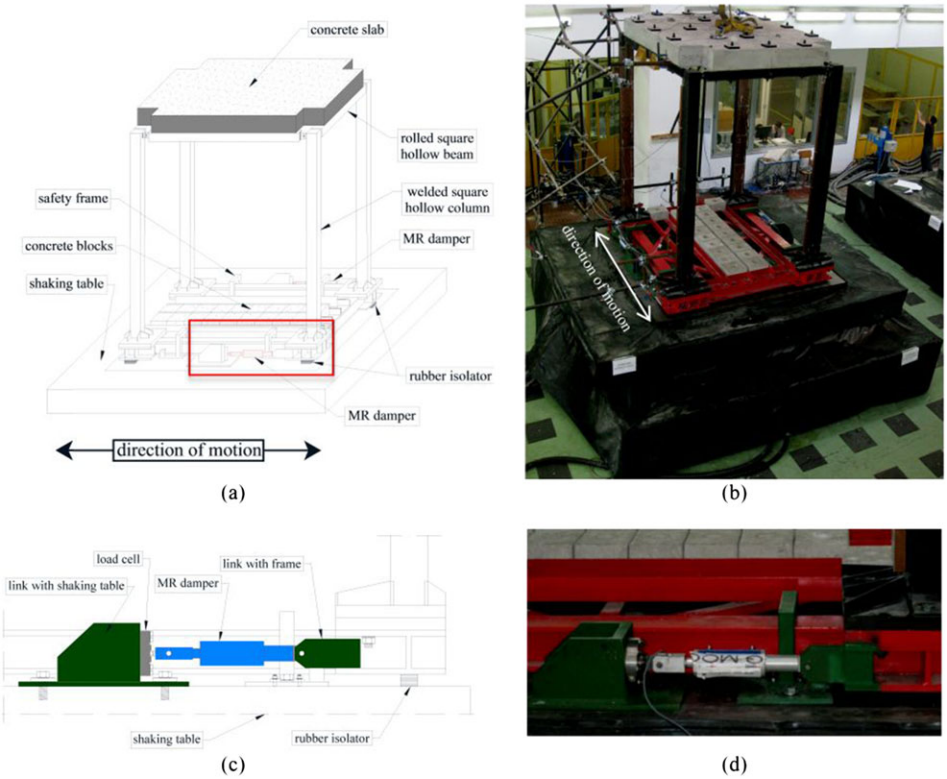

Figure 1. Setup configuration: sketch (a) and general view (b) of the test frame at the Department of Structures for Engineering and Architecture laboratory; sketch (c) and general view (d) of the magnetorheological (MR) device.

DOI: 10.1002/stc

+horizontal steel frame) is approximately 7.8 tons. Four safety frames are added to the setup configuration to prevent the overturning due to excessive displacement (Figure 1(a)).

Two MR dampers, placed on the East and West sides of the setup (Figure 2), were used in this test campaign. They are connected to the frame and shaking table by specially designed steel parts (Figures 1(c) and (d)).

Four rubber bearings placed at the corners of the test frame complete the setup in the test configuration (Figures 1(a) and (c)). The steel frame adopted in the tests simulates a 1:3-scale 1-storey structure. The tests were performed by moving the shaking table in one direction, as indicated in Figures 1(a) and (b).

2.2. Instrumentation

A total of 10 transducers were used to measure the response of the structure during the hybrid tests (Figure 2). Specifically, four laser displacement sensors were placed on the South side of the test setup (two at the top and two at the base of the vertical steel frame) to measure the absolute displacements in the direction of the applied motions. The laser displacement sensors are connected to an external reference steel frame. Accelerations are measured by a total of six triaxial accelerometers. Three accelerometers are located on the concrete slab, two are located at the base of the vertical steel frame in the South-West and South-East corner, and one is located on the shaking table platform (Figure 2).

The sampling frequency of the measured quantities is 200 Hz; during data processing, a 30-Hz low-pass filter was applied to all recorded signals. Finally, piezoresistive load cells mounted at the end of the MR dampers are used to measure the force of the dissipating devices (Figures 1(c) and (d)). Table I summarises the description of all response parameters measured during the tests as well as the adopted sensors, including their position in height and in plan.

3. RUBBER BEARINGS AND MAGNETORHEOLOGICAL DAMPERS

In the following, the adopted rubber bearings and MR dampers are briefly described. Furthermore, the electronic equipment used by the SA control system is introduced, also allowing to highlight specific aspects of this type of experiment that are unusual compared with other types of structural testing.

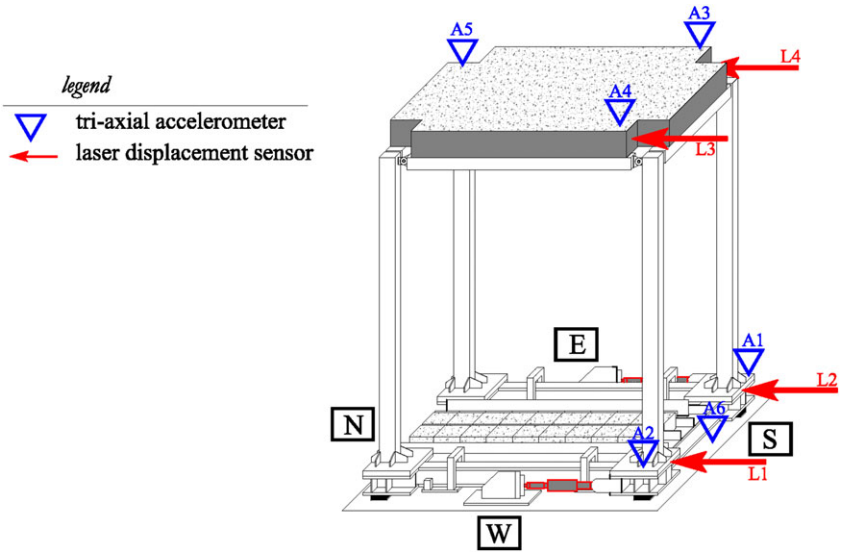

Figure 2. Overview of the instrumentation positioning.

DOI: 10.1002/stc

Table I. Response parameters measured: description, position in height and in plan of the instruments.

Measured parameter	Name	Position in height	Position in plan	Sensor typology
Absolute displacement	L1	Base of the vertical frame	South side	Luchsinger, ±300 mm
	L2	Base of the vertical frame	South side	Luchsinger, ±300 mm
	L3	Top of the vertical frame	South side	Luchsinger, ±300 mm
	L4	Top of the vertical frame	South side	Luchsinger, ±300 mm
Absolute acceleration	A1	Base of the vertical frame	South-East corner	PCB, Triaxial, ±1 g
	A2	Base of the vertical frame	South-West corner	PCB, Triaxial, ±1 g
	A3	Top of the concrete slab	South-East corner	PCB, Triaxial, ±1 g
	A4	Top of the concrete slab	South-West corner	PCB, Triaxial, ±1 g
	A5	Top of the concrete slab	North-East corner	PCB, Triaxial, ±1 g
	A6	Base of the shaking table	South side	PCB, Triaxial, ±1 g
Axial force of device	C1	Base of the shaking table	East side	AEP load cell, ±50 kN
	C2	Base of the shaking table	West side	AEP load cell, ±50 kN

3.1. Description

The rubber bearings used in the tests are named recycled rubber–fibre-reinforced bearings (RR-FRBs). They are made of a low-cost recycled elastomer and are reinforced with fibre sheets. Devices with dimensions of 70 × 70 mm in plane and a thickness of 63 mm were adopted in the tests. Each bearing is manufactured by bonding 12 layers of recycled rubber and 11 bidirectional carbon fibre sheets with a polyurethane adhesive (Figure 3).

The design vertical pressure on the bearings is approximately 3.85 MPa. At a design displacement of 30 mm, the horizontal and vertical stiffness of the bearing are approximately 80 kN/m and 7000 kN/m, respectively. The manufacture of the bearings is very simple. The entire process took only few hours for the curing of the binder. Each bearing is shaped by a table cutting machine that divides a long pad of large dimensions. Currently, only a few prototypes have been produced, and an accurate estimate of the cost of production is not easy. However, it is reasonable to assume that the large-scale production of these bearings for real applications could bring the price up to a hundred euro per isolator. More details can be found in Spizzuoco *et al.* [19].

The MR devices adopted for the tests are two full-scale prototypes (Figure 4) designed and manufactured by the German company Maurer Söhne. The overall dimension of each device is 675 mm (length). A maximum force of 30 kN can be developed along the longitudinal axis, whereas the presence of special spherical pin joints at both ends prevents the development of bending, shear and torsional moments in the piston rod. The dampers have a stroke of ±25 mm. A magnetic circuit composed of coils in series with a total resistance of 3.34 Ω is used

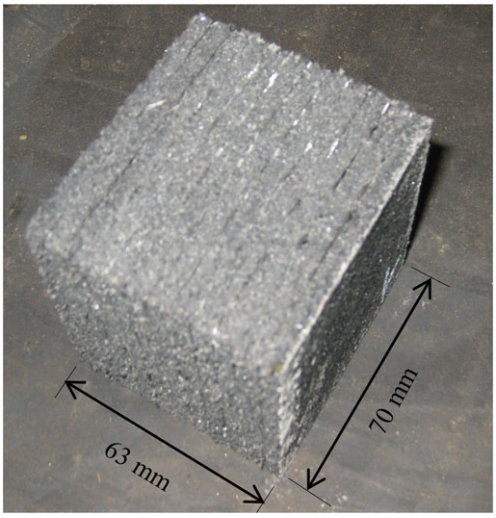

Figure 3. Picture of a rubber bearing.

DOI: 10.1002/stc

Figure 4. One of the two prototype magnetorheological (MR) dampers used in the tests.

to generate the magnetic field in the device. The current in the circuit is provided in the range of $0 \div 3$ A. Detail about mechanical response and dissipative capability of such prototype devices can be found in [20] and [21] respectively.

3.2. Extra equipment for structural control

Additional special electronic equipment was utilised to drive the MR devices in hybrid tests (Figure 5). The equipment includes the following components: (1) a set of two operational power supplies (model BOP 50-4 M from Kepco Inc., New York, USA) featuring an output range of ±50 V, ±4 A (i.e. power source-power sink capabilities of 200 W), which can provide the current needed to feed the circuitry inside the MR device; (2) a 1.0-μF capacitor mounted in parallel with the output for stabilising the current loop operating with inductive loads and measuring both the current and voltage inside the MR damper in real time; (3) the Labview Professional Development System (release 8.5), that is the environment in which the software that acquires and generates all analogue signals involved in the experimental tests was written; (4) a National Instruments (NI) SCC-A10 10-to-1 voltage attenuator for scaling the ±50 V output signal from the power supply to be measured by the acquisition board; (5) an NI PXI 1042 chassis; (6) an NI PXI-8196 RT embedded real-time controller; (7) two NI PXI-6259 data acquisition boards each with 16 analogue inputs and four analogue outputs (±10 V voltage signals, 16-bit resolution and 2800 kHz maximum sampling rate); (8) an NI PXI-4065 digital multimeter for measuring the current in the damper's circuit; and (9) two NI BNC-2110 connector blocks.

The MR dampers have two parallel and independent configurations of sensors, cables, control algorithms and power supplies. For on-line control, the sampling frequency of relevant quantities was set to 1 kHz. Signals have been low-pass processed using a second-order Butterworth filter and a 30 Hz cutting frequency. Because of structural symmetry, the data recorded for each damper are practically identical; therefore, in the following, we will refer to either of the two sides.

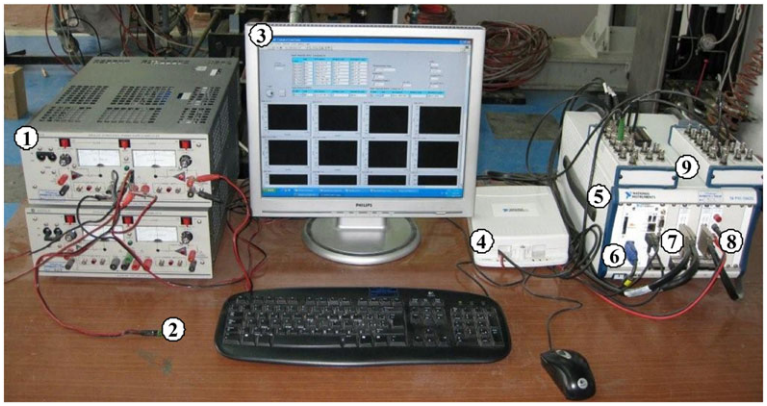

Figure 5. Electronic equipment for acquisition and control for the Joint Experimental Testing on Base Isolation Systems experimental tests: power supplies (1), 1.0 μF capacitor (2), Labview software (3), voltage attenuator (4), National Instruments chassis (5), real-time National Instruments CPU (6), data acquisition board (7), digital multimeter (8) and connector block (9).

DOI: 10.1002/stc

4. INPUT AND TESTING PROTOCOL

A set of three acceleration time histories was used for the tests. The earthquake accelerograms were derived from the experimental campaign on isolated structures performed by Calabrese *et al.* in 2014 [16]. In particular, spectrum-matching accelerograms were used for the tests by selecting a set of seven waveforms compatible with the Italian Seismic Code [22] according to the code provision described in [23,24]. Only three more severe earthquakes (Bingol, Campano-Lucano, Montenegro) out of the seven selected in Calabrese *et al.* [16] were used in the present experimental tests. Three is the minimum number of events to be considered, according to many standards, when time history analyses are adopted to characterise the seismic response of a given structure. Time constraints did not allow implementing additional shaking table analyses, each requiring an intense preliminary activity to ensure being able to perform the test in a safe way, taking into account the unusual behaviour of the adopted low-cost bearings. Given a geometry scale factor of the test frame of 1/3, to satisfy the dynamic similitude requirements, the selected earthquakes have been compressed in time by the same scale factor. The magnitudes of the signals are also scaled (see SF in Table II) to obtain a peak ground acceleration equal to 2.55 m/s^2 for all time histories. The maximum value of the acceleration scale factors is 1.01, the minimum is 0.80 and the mean is 0.89. The acceleration time-history inputs for the shaking table tests are shown in Figure 6. Table II lists the main parameters of these ground motions and demonstrates that the values of peak ground acceleration for all of the events are equal (2.55 m/s^2).

The experimental activity included 12 tests. Table III shows their characteristics. In tests #1, #2 and #3, the frame is isolated by rubber bearings only (BI) and subject to the Bingol, Campano-Lucano and Montenegro earthquakes, respectively, without supplemental dampers. These tests form the basis of a comparison for evaluating the effectiveness of the proposed hybrid BI system. Subsequently, MR dampers are added to the initial configuration to reduce the base displacements. In tests #4, #5 and #6, the MR dampers are not fed with a current (passive OFF configuration), thus corresponding to a moderate level of supplemental damping. A high level of supplemental damping was adopted for tests #7 to #9, where the current fed to the dampers is 0.4 A (passive ON configuration). Tests #10, #11 and #12 refer to devices operated in a semi-active manner according to a properly designed algorithm (SA configuration).

5. SEMI-ACTIVE CONTROL ALGORITHM. EVALUATION OF ADDITIONAL DAMPING

The previously described structural mock up can be modelled as a 2-DOF system. A preliminary set of identification tests allowed characterising the tested structure as follows: $m_2 = 4625$ kg, $m_1 = 3208$ kg, $k_2 = 3051000$ N/m, $k_1 = 606000$ N/m, $c_2 = 1176$ Ns/m, $c_1 = 12250$ Ns/m. With reference to the preceding values, mass, damping and stiffness matrices are organised as follows:

$$\mathbf{M} = \begin{bmatrix} m_1 & 0 \\ 0 & m_2 \end{bmatrix} \quad \mathbf{C} = \begin{bmatrix} c_1 + c_2 & -c_2 \\ -c_2 & c_2 \end{bmatrix} \quad \mathbf{K} = \begin{bmatrix} k_1 + k_2 & -k_2 \\ -k_2 & k_2 \end{bmatrix} \tag{1}$$

The equations of free motion of the bare frame, that is, without the influence of MR dampers, can be written as usual:

$$\mathbf{M}\ddot{\mathbf{x}} + \mathbf{C}\dot{\mathbf{x}} + \mathbf{K}\mathbf{x} = 0 \tag{2}$$

where $\mathbf{x} = [x_1\ x_2]^{\mathrm{T}}$ is the two-component vector of the system displacements relative to the base. Each component is a scalar function of time; however, the time dependence will be explicitly written only when strictly needed. In the typical hypothesis of neglecting damping, the main modal parameters are

Table II. Selected ground motion, specifics and significant parameters.

Earthquake name	Waveform ID	Station ID	Date [dd/mm/yyyy]	SF	PGA [m/s^2]	PGV [cm/s]	PGD [cm]
Bingol (BIN)	7142ya	ST539	01/05/2003	0.87	2.55	18.29	3.25
Campano-Lucano (CAM)	290ya	ST96	23/11/1980	0.80	2.55	44.10	16.20
Montenegro (MON)	200ya	ST68	15/04/1979	1.01	2.55	12.87	9.60

PGV, peak ground velocity; PGD, peak ground displacement.

DOI: 10.1002/stc

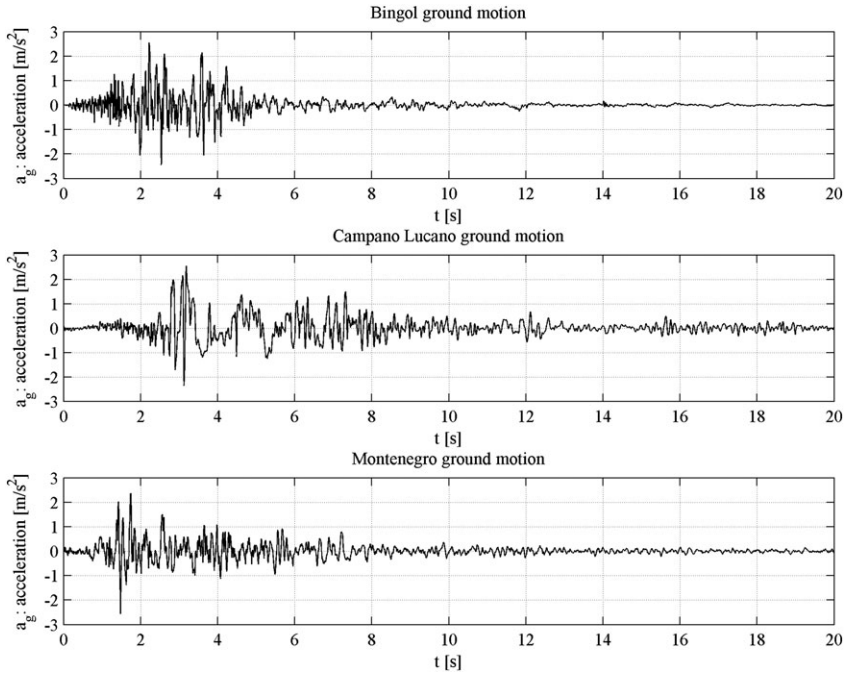

Figure 6. Acceleration time-history inputs for shaking table tests.

modal periods $T_1 = 0.74\,\text{s}; \qquad T_2 = 0.15\,\text{s}$

modal shapes $$\mathbf{\Phi} = \begin{bmatrix} \varphi_{1,1} & \varphi_{1,2} \\ \varphi_{2,1} & \varphi_{2,2} \end{bmatrix} = \begin{bmatrix} 0.891 & -1.620 \\ 1.000 & 1.000 \end{bmatrix} = \begin{bmatrix} 0.891\angle 0° & 1.620\angle 180° \\ 1.000\angle 0° & 1.000\angle 0° \end{bmatrix}$$

Modal shapes are normalised so that the second row component (corresponding to DOF n. 2) is set to 1. The first eigenvector clearly shows that the isolation effect is partial and with a significant structural strain. An alternative representation of the modal shapes (modulus and phase) is shown for comparison with what follows. In this case, the 180° phase delay of the second component of the second mode corresponds to the minus sign in the typical representation of mode shapes in the time domain. Modal periods T_i fit the experimentally evaluated counterparts reasonably well.

Table III. Experimental activity.

Setup configuration	Test no.	Earthquake	Max current in MR dampers [A]
Base isolation	1	BIN	—
	2	CAM	
	3	MON	
Hybrid base isolation with MR dampers used as passive devices (Passive ON/OFF)	4	BIN	0
	5	CAM	
	6	MON	
	7	BIN	0.40
	8	CAM	
	9	MON	
Hybrid base isolation with MR dampers used as semi-active devices	10	BIN	0.40
	11	CAM	
	12	MON	

MR, magnetorheological; BIN, Bingol; MON, Montenegro; CAM, Campano-Lucano.

DOI: 10.1002/stc

The linear system of Eq. (2) (two time-invariant second-order differential equations) can also be written as a set of four linear, time-invariant, first-order differential equations in the state space representation:

$$\dot{\mathbf{z}} = \mathbf{A}\,\mathbf{z} \tag{3}$$

where

$$\mathbf{A} = \begin{bmatrix} \mathbf{0}_{2\times2} & \mathbf{I}_{2\times2} \\ -\mathbf{M}^{-1}\mathbf{K} & -\mathbf{M}^{-1}\mathbf{C} \end{bmatrix} \quad (\dim \mathbf{A} = 4\times4) \tag{4}$$

and

$$\mathbf{z} = [\mathbf{x} \quad \dot{\mathbf{x}}]^{\mathrm{T}} = [x_1 \quad x_2 \quad \dot{x}_1 \quad \dot{x}_2]^{\mathrm{T}} \tag{5}$$

is the system state. By explicitly considering damping (inherent structural damping and that associated to the isolation devices), the main modal parameters computed in the state space domain are

modal periods $T_1 = 0.74\,\mathrm{s}$; $T_2 = 0.15\,\mathrm{s}$

modal damping ratios $\zeta_1 = 8{,}0\%$; $\zeta_2 = 3{,}7\%$

modal shapes $\boldsymbol{\Psi}^* = [\boldsymbol{\psi}_1 \quad \boldsymbol{\psi}_2] = \begin{bmatrix} 0.892\angle1^\circ & 1.620\angle175^\circ \\ 1.000\angle0^\circ & 1.000\angle0^\circ \end{bmatrix}$

Compared with the undamped analysis, the BI structure without supplemental dampers includes an insignificant phase between the components of the first eigenvector and a reduction in the phase between the components of the second eigenvector, whereas absolute values are comparable. The addition of a significant amount of damping should correspond to a 'degradation' of modal shapes, that is, to higher values of phase between the components of each mode. Specifically, benefits associated with the increase in damping would be reduced or vanish because of the modal modifications induced by damping.

By considering the force f of the dampers, Eq. (2) becomes

$$\mathbf{M}\ddot{\mathbf{x}} + \mathbf{C}\dot{\mathbf{x}} + \mathbf{K}\mathbf{x} - [f \quad 0]^{\mathrm{T}} = 0 \tag{6}$$

or

$$\mathbf{M}\ddot{\mathbf{x}} + \mathbf{C}\dot{\mathbf{x}} + \mathbf{K}\mathbf{x} = \mathbf{p}\,f \quad \left(\mathbf{p} = [1 \quad 0]^{\mathrm{T}}\right) \tag{7}$$

Accordingly, the equation of free vibrations in the state space becomes

$$\dot{\mathbf{z}} = \mathbf{A}\,\mathbf{z} + \mathbf{b}\,f \tag{8}$$

where

$$\mathbf{b} = \begin{bmatrix} \mathbf{0}_{2\times1} \\ \mathbf{M}^{-1}\mathbf{l} \end{bmatrix} \quad (\dim \mathbf{b} = 4\times1) \tag{9}$$

If the force f is provided by a linear viscous damper with constant c, that is,

$$f = -c\cdot\dot{x}_1 = -\mathbf{C}_d\cdot\dot{\mathbf{x}} \tag{10}$$

where

$$\mathbf{C}_d = \begin{bmatrix} c & 0 \\ 0 & 0 \end{bmatrix} \tag{11}$$

Eq. (7) could be written as

$$\mathbf{M}\ddot{\mathbf{x}} + (\mathbf{C} + \mathbf{C}_d)\,\dot{\mathbf{x}} + \mathbf{K}\mathbf{x} = 0 \tag{12}$$

and Eq. (8) would become

$$\dot{\mathbf{z}} = \mathbf{A}_{\mathrm{CL}}\,\mathbf{z} \tag{13}$$

where

DOI: 10.1002/stc

$$\mathbf{A}_{\mathrm{CL}} = \begin{bmatrix} \mathbf{0}_{2\times2} & \mathbf{I}_{2\times2} \\ -\mathbf{M}^{-1}\mathbf{K} & -\mathbf{M}^{-1}(\mathbf{C}+\mathbf{C}_d) \end{bmatrix} \tag{14}$$

The effect of the additional dissipation provided by MR dampers is analysed in terms of equivalent viscous damping [25]. When currents of 0 and 0.4 A are applied, each MR damper corresponds to a linear equivalent damper with a viscous constant that is approximately equal to $c_0 = 30$ kN s/m and $c_{0.4} = 60$ kN s/m in the cases of Bingol and Montenegro base accelerations, respectively, where the maximum velocities of the base with respect to the ground are approximately 0.09 m/s. For the Campano-Lucano accelerogram, where the maximum recorded velocities are close to 0.19 m/s, the equivalent linear viscous coefficients are approximately $c_0 = 20$ kN s/m and $c_{0.4} = 40$ kN s/m. The complex modal analysis corresponding to the passive configurations of MR dampers (current set to 0 and 0.40 A) yields the results shown in Table IV, where data corresponding to the BI structure without dampers are also presented for comparison.

As shown in the next section, the addition of a high level of damping to the base of the structure corresponds, as expected, to a significant reduction in base displacements at the cost of a general increase in both interstory drift and peak accelerations. In an attempt to overcome the undesirable side effects of the additional damping, in a further series of tests, the current in the MR devices was continuously varied according to a SA control scheme.

Generally speaking, in a base-isolated n-DOF structure with m independent actuators, the equations of free motion can be represented as

$$\mathbf{M}\ddot{\mathbf{x}} + \mathbf{C}\dot{\mathbf{x}} + \mathbf{K}\mathbf{x} = \mathbf{P}\,\mathbf{f} \tag{15}$$

where $\mathbf{M}$, $\mathbf{C}$ and $\mathbf{K}$ are the mass, damping and stiffness matrices, respectively, and $\mathbf{P}$ is the $n \times m$ allocation matrix of the control forces f_{di} collected in the control vector $\mathbf{f}_d$. If is assumed that the SA forces in the dampers '$\mathbf{f}_d$' have specific values '$\mathbf{f}_u$', for example, functions of the system's state through a gain matrix $\mathbf{G}$

$$\mathbf{f}_u(t) = -\mathbf{G}\cdot\mathbf{z}(t) \tag{16}$$

then the state-space representation of the closed feedback loop n-DOF structural system under free vibration becomes

$$\dot{\mathbf{z}} = \mathbf{A}\,\mathbf{z} + \mathbf{B}\,\mathbf{f}_u = \mathbf{A}\,\mathbf{z} + \mathbf{B}\,(-\mathbf{G}\,\mathbf{z}) = (\mathbf{A} - \mathbf{B}\,\mathbf{G})\,\mathbf{z} = \mathbf{A}_{\mathrm{CL}}\,\mathbf{z} \tag{17}$$

Eigenvalues and eigenvectors of $\mathbf{A}_{\mathrm{CL}}$ (summarising the properties of the closed-loop controlled system) are different from those of $\mathbf{A}$; in other words, frequencies, damping ratios and modal shapes of the controlled system are different from those of the uncontrolled system. Therefore, the question arises if modal parameters can be modified in a more favourable way. An answer to this question was most likely first introduced by Moore [26] and subsequently explored by many scholars, but the authors are unaware of any application to the particular case of SA-controlled BI structures. In this latter case, it would be desirable to have an initial modal shape that resembles the motion of a rigid body above isolators with a high-damping ratio, whereas higher modes should have participation factors of close to 0.

Let us assume that a matrix $\mathbf{G}$ does exist such that $s_{d,i}$ and $\boldsymbol{\psi}_{d,i}$ are the desired eigenvalue and eigenvector of the ith mode of the closed-loop (CL) system. When the CL system vibrates according to that mode, the system's state varies proportionally to the displacements and velocities described by the corresponding eigenvector

$$\mathbf{z}(t) = \boldsymbol{\psi}_{d,i}\cdot e^{s_{d,i}t} \tag{18}$$

and in this case, the desired control forces $\mathbf{f}_{ui}$ can be expressed as

$$\mathbf{f}_{ui}(t) = \mathbf{u}_i\cdot e^{s_{d,i}t} = -\mathbf{G}\,\mathbf{z}(t) = -\mathbf{G}\,\boldsymbol{\psi}_{d,i}\cdot e^{s_{d,i}t} \tag{19}$$

Let us evaluate the product $\mathbf{A}_{\mathbf{CL}}\,\boldsymbol{\psi}_{d,i}$:

$$\mathbf{A}_{\mathrm{CL}}\,\boldsymbol{\psi}_{d,i} = (\mathbf{A} - \mathbf{B}\,\mathbf{G})\,\boldsymbol{\psi}_{d,i} = \mathbf{A}\,\boldsymbol{\psi}_{d,i} + \mathbf{B}\,\left(-\mathbf{G}\,\boldsymbol{\psi}_{d,i}\right) = \mathbf{A}\,\boldsymbol{\psi}_{d,i} + \mathbf{B}\,\mathbf{u}_i \tag{20}$$

Given $s_{d,i}$ and $\boldsymbol{\psi}_{d,i}$, that is, an eigenvalue and the corresponding eigenvector of $\mathbf{A}_{\mathrm{CL}}$, the same product is also equal to

DOI: 10.1002/stc

Table IV. Modal parameters of passive configurations.

	BI		Passive off $c_0 = 20$ kNs/m		Passive off $c_0 = 30$ kNs/m		Passive on $c_{0.4} = 40$ kNs/m		Passive on $c_{0.4} = 60$ kNs/m	
	First mode	Second mode	First mode	Second mode	First mode	Second mode	First mode	Second mode	First mode	Second mode
Period	0.74 s	0.15 s	0.73 s	0.15 s	0.71 s	0.16 s	0.69 s	0.16 s	0.64 s	0.18 s
Damping ratio	8.0%	3.7%	35%	13%	49%	18%	64%	23%	99%	31%
Modal shape	$0.89\angle 1°$	$1.62\angle 175°$	$0.91\angle 5°$	$1.58\angle 156°$	$0.94\angle 6°$	$1.53\angle 147°$	$0.98\angle 7°$	$1.47\angle 137°$	$1.15\angle 6°$	$1.27\angle 117°$
	$1.00\angle 0°$	$1.00\angle 0°$	$1.00\angle 0°$	$1.00\angle 0°$	$1.00\angle 0°$	$1.00\angle 0°$	$1.00\angle 0°$	$1.00\angle 0°$	$1.00\angle 0°$	$1.00\angle 0°$

DOI: 10.1002/stc

$$\mathbf{A}_{\mathrm{CL}}\ \boldsymbol{\psi}_{d,i} = s_{d,i}\ \boldsymbol{\psi}_{d,i} \tag{21}$$

By combining Eqs. (20) and (21),

$$\mathbf{A}_{\mathrm{CL}}\ \boldsymbol{\psi}_{d,i} = \mathbf{A}\ \boldsymbol{\psi}_{d,i} + \mathbf{B}\ \mathbf{u}_i = s_{d,i}\ \boldsymbol{\psi}_{d,i} \tag{22}$$

or

$$\mathbf{B}\ \mathbf{u}_{\mathrm{i}} = \left(s_{d,i}\ \mathbf{I} - \mathbf{A}\right)\ \boldsymbol{\psi}_{d,i} \tag{23}$$

and finally,

$$\boldsymbol{\psi}_{d,i}\ = \left[\left(s_{d,i}\ \mathbf{I} - \mathbf{A}\right)^{-1}\mathbf{B}\right]\ \mathbf{u}_{\mathrm{i}} = \mathbf{H}_i\ \mathbf{u}_i \quad \left(\dim \mathbf{H}_i = 2n{\times}m\right) \tag{24}$$

Equation (24) shows the relations among the desired eigenvalue $s_{d,i}$ and eigenvector $\boldsymbol{\psi}_{d,i}$; the matrix of the original, uncontrolled system $\mathbf{A}$; and the desired parameters of the ith vibration mode, that is, the control force capable of vibrating the controlled system according to a desired modal shape. Should the matrix $\mathbf{H}_i$ be invertible, the calculation of the control force $\mathbf{u}_i$ would be straightforward. However, $\mathbf{H}_i$ is generally not invertible. An approximate approach to solving Eq. (24) for $\mathbf{u}_i$ is to consider the pseudo-inverse matrix $\hat{\mathbf{H}_i}$ of $\mathbf{H}_i$. In this case, the calculation of $\mathbf{u_i}$ can be performed as follows:

$$\mathbf{u}_i = \mathbf{H}_i\boldsymbol{\psi}_{d,i}\ = \left[\left(\mathbf{H}_i^{\mathrm{T}}\ \mathbf{H}_i\right)^{-1}\mathbf{H}_i^{\mathrm{T}}\right]\ \boldsymbol{\psi}_{d,i} \tag{25}$$

Obviously, using the approximation expressed in Eq. (25), the eigenvector $\boldsymbol{\psi}_{CL,i}$ of the CL system will be similar but not exactly equal to the desired $\boldsymbol{\psi}_{d,i}$:

$$\boldsymbol{\psi}_{CL,i} = \mathbf{H}_i\ u_i \cong \boldsymbol{\psi}_{d,i} \tag{26}$$

Finally, by selecting the desired parameters $s_{d,i}$ and $\boldsymbol{\psi}_{d,i}$ of each mode to be reshaped, it is possible to calculate the corresponding values of the desired control force $\mathbf{u}_i$ and the resulting CL eigenvector $\boldsymbol{\psi}_{CL,i}$, which are to be collected in the matrices $\mathbf{U}$ and $\boldsymbol{\psi}_{CL}$, respectively:

$$\begin{aligned}\mathbf{U}\ &= \left[\mathbf{u}_1 \quad \mathbf{u}_2 \quad \ldots \quad \mathbf{u}_{2n}\right];\ \boldsymbol{\Psi}_{CL} \\ &= \left[\boldsymbol{\psi}_{CL,1} \quad \boldsymbol{\psi}_{CL,2} \quad \ldots \quad \boldsymbol{\psi}_{CL,2n}\right] \quad \left(\dim \mathbf{U} = m{\times}2n;\ \dim \boldsymbol{\Psi}_{CL} = 2n{\times}2n\right)\end{aligned} \tag{27}$$

Recalling Eq. (16), it becomes

$$\mathbf{U} = -\mathbf{G}\ \boldsymbol{\Psi}_{CL} \tag{28}$$

and the gain matrix $\mathbf{G}$ can be found as

$$\mathbf{G} = -\ \mathbf{U}\ \boldsymbol{\Psi}_{CL}^{-1} \tag{29}$$

Once $\mathbf{G}$ is calculated through Eq. (29), the corresponding control force $\mathbf{f}_u$, defined by Eq. (16), can approximately transform the original structure so that it has the desired modal properties:

- frequency and damping ratio of each selected mode (through s_i) and
- modal shapes (through $\boldsymbol{\psi}_{d,i}$).

It is worth noting that the previously described procedure also works if only a portion of a CL eigenvector is desired to have a given shape. In other words, the selection can also be applied to some or all CL eigenvectors. Because of the previously introduced approximate calculations, the less demanding the eigenvector selection, the more accurate the results, that is, the closer the CL and desired eigenvectors.

Therefore, provided that more than one independent controller is available and that the positioning of such controllers yields a controllable system, for a feedback-controlled base-isolated structure, it is thus possible to directly design the modal behaviour in terms of both modal frequencies and damping ratio and modal shapes. When there is only one controller available, as in the case of the experimental activity described herein, the previously described procedure cannot be applied. However, the pole placement technique also modifies, through $\mathbf{G}$, the CL system matrix and, in turn, its complex eigenvectors (i.e. the modal shapes of the base-isolated structure). Therefore, when the desired control force $\mathbf{u}$ is designed using Eq. (16) to obtain given values of periods of vibration and modal damping ratios for the CL system, the modal shapes of the controlled system also change compared with the original,

DOI: 10.1002/stc

uncontrolled system. Based on a trial-and-error iterative procedure, the author produced the following feedback control law:

$$\begin{aligned} u &= -\mathbf{G}\cdot\mathbf{z} \\ &= -104\ \text{kN/m}\cdot x_1\ \text{m} + 104\ \text{kN/m}\cdot x_2\ \text{m} - 28.8\ \text{kN}\cdot\text{s/m}\cdot\dot{x}_1\ \text{m/s} + 2.36\ \text{kN}\cdot\text{s/m}\cdot\dot{x}_2\ \text{m/s} \end{aligned} \quad (30)$$

The resulting CL system includes the following modal parameters:

complex eigenvalues	$s_1 = -2.12 \pm \text{j}\ 8.23\ \text{rad/s};$	$s_2 = -4.57 \pm \text{j}\ 41.3\ \text{rad/s}$
modal periods	$T_1 = 0.74\ \text{s};$	$T_2 = 0.15\ \text{s}$
modal damping ratios	$\zeta_1 = 25{,}0\%;$	$\zeta_2 = 11{,}0\%$
modal shapes	$\boldsymbol{\Psi}^* = [\,\boldsymbol{\psi}_1 \quad \boldsymbol{\psi}_2\,] = \begin{bmatrix} 0.905\angle 1^\circ & 1.650\angle 161^\circ \\ 1.000\angle 0^\circ & 1.000\angle 0^\circ \end{bmatrix}$	

The control law described by Eq. (30) would require a force actuator to be applied to the BI structural system. When a passive, although smart, damper is adopted to exert the control force, rather than an actuator, it is not always possible to force the damper to react with the desired force u. The actual force f in the damper is reactive by nature, and thus, when f and u have opposite signs, the only possibility is to minimise f. Recalling that the actual force in an SA MR damper is non-linearly proportional to the current i feeding the coils inside the damper and to the corresponding magnetic field, the semi-active control algorithm must drive the damper so that the current that is feeding the circuit inside the device is varied at each time step.

6. RESULTS AND DISCUSSION

Preliminary tests were conducted to evaluate the maximum strain of low-cost BI devices. The steel frame, only isolated by rubber bearings, was subjected to 1 Hz sinusoidal signals and increasing amplitude from 10 to 30 mm. The bearings collapsed at an amplitude of 20 mm that for a thickness of 63 mm means a displacement/thickness ratio about of 30%. This proves that the use of additional devices to limit the strain is important in a possible application of this low-cost technology. During the tests, MR dampers were used in three different manners: passive OFF (low supplemental damping), passive ON (high supplemental damping) and semi-active (variable supplemental damping). The results were compared in terms of interstory drifts as well as base displacements and roof accelerations.

6.1. Test results

For each earthquake, two different currents, 0 and 0.40 A, were used to feed the MR dampers under passive conditions and correspond to command signals of 0 and 1 V (the gain of the power supply is approximately 2.5 V/A (input over output)). For the semi-active configuration, the maximum current to the MR dampers was again set to 0.4 A. Table V reports the maximum response parameters in terms of base displacements, interstory drifts and accelerations of the upper level. Figure 7 shows the same data by assuming as a reference the response level of the BI configuration.

The experimental data show that a high level of additional damping at the base (passive ON), corresponding to a damping ratio of the first mode from 60% to critical, may significantly reduce, as expected, base displacements (Figure 7(a)) but imply higher drifts and top accelerations compared with a configuration featuring a lower level of additional damping (Figure 7(b) and (c)). The only exception is the Campano-Lucano signal, for which the passive ON condition corresponds to a modal shape modification (see Table IV at $c_0 = 40$ kNs/m) that can obtain a nearly perfect isolation scheme (the moduli of the first and second component of the first complex eigenvector are very similar).

The base displacement reduction achieved by the passive ON control system can be close to 60% (Figure 7(a)). However, the response reduction provided in terms of roof accelerations can also be negligible or even negative, as is seen for the Campano-Lucano and Montenegro earthquakes (Figure 7 (c)). In this case, the use of an SA strategy is crucial to invert this negative result and to obtain a

DOI: 10.1002/stc

Table V. Peak response parameters: comparison among different setup configurations.

Earthquake	Test no.	Setup configuration	i_{max} [A]	Max base displacement [mm]	Max interstory drift [mm]	Max top acceleration [m/s^2]
BIN	1	BI	—	8.78	5.52	2.19
	4	Passive OFF	0	7.30	3.79	1.84
	7	Passive ON	0.40	4.74	5.02	1.95
	10	SA	0.40	6.44	4.98	2.00
	—	Fixed base	—	—	6.96	3.90
CAM	2	BI	—	22.17	9.66	2.40
	5	Passive OFF	0	19.82	7.11	2.42
	8	Passive ON	0.40	8.15	6.40	2.38
	11	SA	0.40	17.81	7.68	2.32
	—	Fixed base	—	—	8.99	5.02
MON	3	BI	—	9.04	5.69	2.02
	6	Passive OFF	0	6.78	3.78	1.63
	9	Passive ON	0.40	4.11	4.15	2.46
	12	SA	0.40	6.24	3.57	1.68
	—	Fixed base	—	—	5.51	3.04

BIN, Bingol; MON, Montenegro; CAM, Campano-Lucano; SA, semi-active.

response reduction for all of the investigated parameters (Table V). Note that the SA configuration yields a response reduction in terms of base displacements that lies halfway between the passive cases of high and low damping (Figure 7(a)).

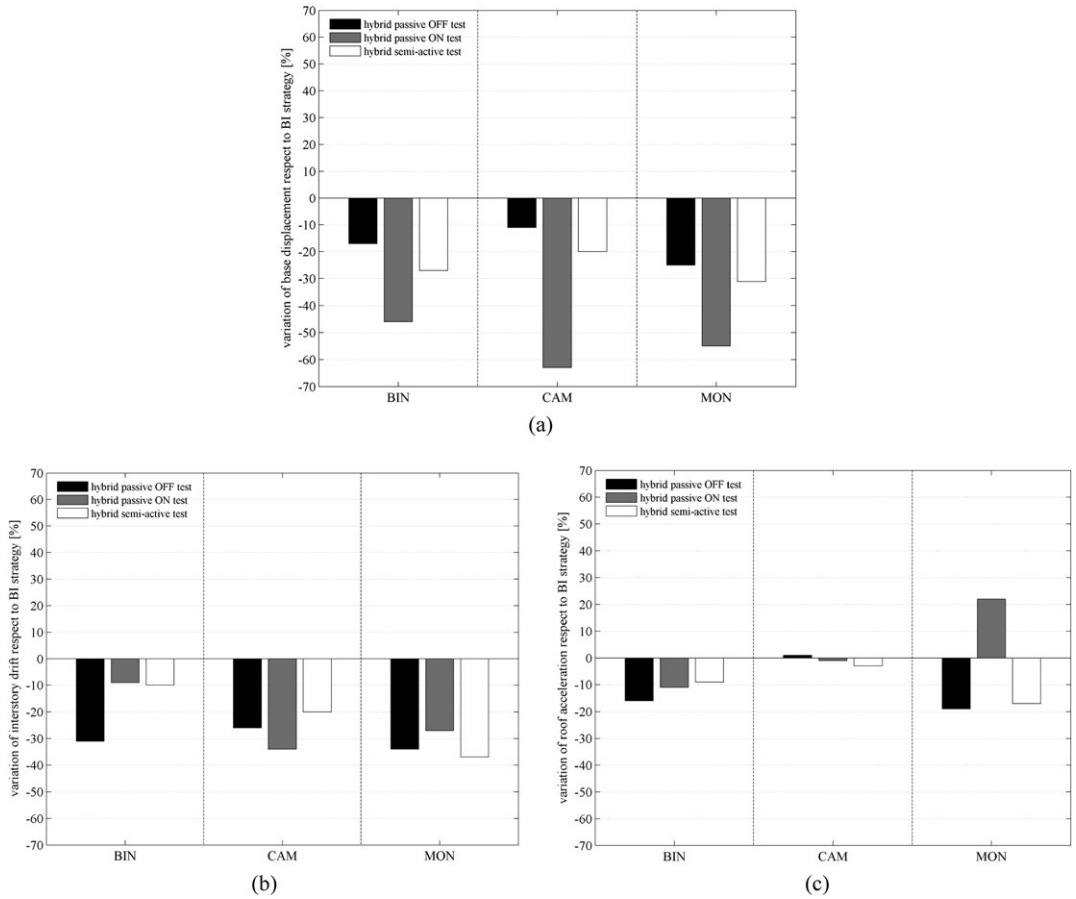

Figure 7. Comparison in terms of base displacements (a), interstory drifts (b), and roof accelerations (c) of different setup configurations. BIN, Bingol; CAM, Campano-Lucano; MON, Montenegro.

DOI: 10.1002/stc

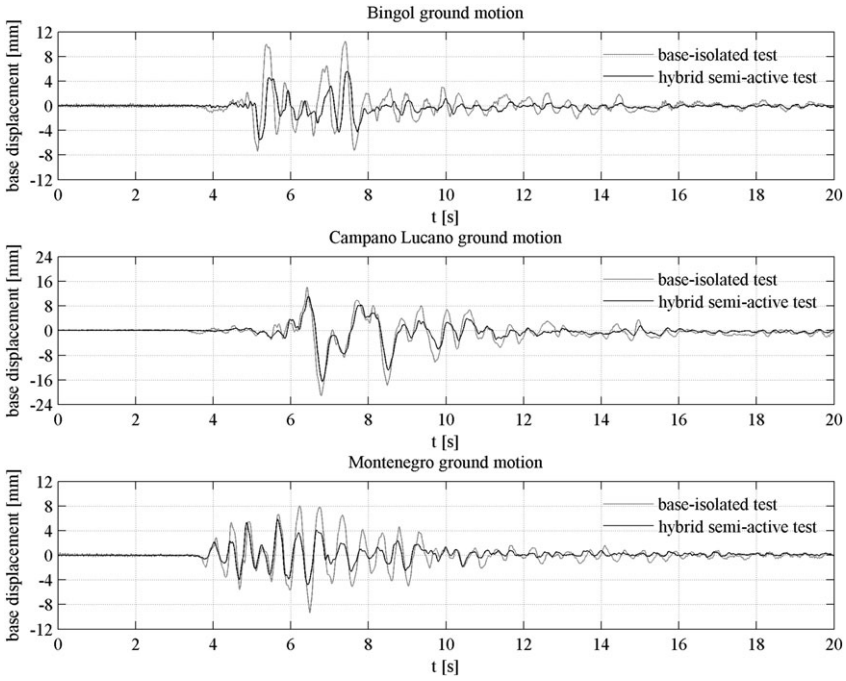

Figure 8. Base displacement time histories: comparison of the 'base isolated only' and hybrid semi-active responses.

All of the tests were also analysed in terms of time-history displacements. Figure 8 shows the responses of the structure when subject to the Bingol, Campano-Lucano and Montenegro earthquakes to enable a comparison of the base displacements of the BI and SA configurations. The figure clearly shows the maximum response reduction associated with the SA configuration as well as a general reduction in the structural demand in terms of base displacements.

The maximum response parameters in terms of interstory drifts and top accelerations of the fixed-base structure were analytically calculated. The results are reported in Table V and confirm the effectiveness of the proposed hybrid technology. In particular, the response in terms of top floor accelerations shows, for hybrid solutions, a strong reduction with respect to the fixed-base structure. For the interstory drift, the tests indicate different performances for the Campania and Montenegro records (Campano-Lucano and Montenegro). Small increases, for tests performed on the BI structure with respect to the fixed-base structure, were observed. In these cases, the role of MR dampers is crucial for enhancing the seismic performance of the structure.

7. CONCLUSIONS

The main results of an experimental study on a base-isolated structure that exploits low-cost rubber isolators equipped with supplemental variable dampers have been presented. As traditional isolators, low-cost rubber bearings have their weak point on large displacements. In particular, for sites requiring large design displacements (e.g. in epicentral areas), there is a need to bound the strain of such isolators to an acceptable level. This is crucial to enable the possible application of this low-cost technology. The addition of passive dampers at the base of an isolated structure effectively reduces the base displacements and, in turn, the strain in the isolators. However, this reduction is generally obtained at a cost of reducing the benefits of isolation at upper levels in terms of both interstory drifts and peak accelerations, and the greater the supplemental damping provided at the base, the greater the reduction in effectiveness of the isolation system at the upper levels. Herein, the adoption of a SA control system driving MR dampers in real time has been proved being able to yield a reduction in base displacements without producing undesired effects in terms of the response of the upper levels.

About the economic convenience of using the proposed hybrid technique to protect structures against severe earthquakes, a case by case evaluation has to be done because the response cannot be generalised. Of course, using MR dampers and SA control partially reduces the advantage of installing

DOI: 10.1002/stc

low-cost rubber bearings. However, a fair economic analysis should take into account that (i) often the BI system is installed with the addition of viscous dampers, with their additional cost; (ii) according to the dimensions in plan of the structure to be protected (i.e. according to the number of columns), the number of isolators grows proportionally, while the number of SA devices can be limited to a few (e.g. a couple) for each horizontal direction; and (iii) the enhancement of the seismic safety of the structural system when the hybrid control is adopted instead of a pure passive BI technique, among the benefits of the proposed technology.

The SA controller has been designed for this specific application, aiming at improving the performance the BI system alone would lead to. As future development of this work, the authors are working on a numerical model of the structure, first to simulate the available experimental results, then to make prediction about the dynamic response of the same structure to different seismic loads or when controlled with alternative control logics.

ACKNOWLEDGEMENTS

This research study is funded by the Italian Department of Civil Protection under the framework of the national project DPC – ReLUIS 2010–2013 and by the University of Naples "Parthenope" with a grant within the call "Support for Individual Research for the 2015-17 Period" issued by Rectoral Decree no. 727/2015. The support of both is gratefully acknowledged. The technical support provided by Eng. Francesco Trinchillo during the shake table tests at the University of Naples, Federico II, Italy, is highly appreciated.

REFERENCES

1. Patil SJ, Reddy GR. State of art review – base isolation systems for structures. *International Journal of Emerging Technology and Advanced Engineering* 2012; **2**(7):438–453.
2. Chopra AK. *Dynamics of Structures: Theory and Applications to Earthquake Engineering*. Prentice Hall, Inc., Pearson Education: Upper Saddle River, New Jersey, 2011. ISBN:9780131561748.
3. Pant DR, Wijeyewickrema AC. Structural performance of a base-isolated reinforced concrete building subjected to seismic pounding. *Earthquake Engineering and Structural Dynamics* 2012; **41**:1709–1716.
4. Kelly JM. The role of damping in seismic isolation. *Earthquake Engineering and Structural Dynamics* 1999; **28**(1):3–20.
5. Makris N. Rigidity- plasticity- viscosity: can be electrorheogical dampers protect base-isolated structures from near-source ground motions? *Earthquake Engineering and Structural Dynamics* 1997; **26**:571–591.
6. Li H, Ou J. A design approach for semi-active and smart base-isolated buildings. *Structural Control and Health Monitoring* 2006; **13**(2-3):660–681.
7. Madden GJ, Symans MD, Wrongprasert N. Experimental verification of seismic response of building frame with adaptive sliding base isolation system. *Journal of Structural Engineering* 2002; **128**(8):1037–1045.
8. Lin PY, Roschke PN, Loh CH. Hybrid base isolation with magnetorheological damper and fuzzy control. *Structural Control and Health Monitoring* 2007; **14**(3):384–405.
9. Yoshioka H, Ramallo JC, Spencer BF. "Smart" Base isolation strategies employing magnetorheological dampers. *Journal of Engineering Mechanics* 2002; **128**(5):540–551.
10. Shook D, Lin PY, Lin TK, Roschke PN. A comparative study in the semi-active control of isolated structures. *Smart Materials and Structures* 2007; **16**(4):1433–1446.
11. Kim HS, Roschke PN, Lin PY, Loh CH. Neuro-fuzzy model of hybrid semi-active base isolation system with FPS bearings and an MR damper. *Engineering Structures* 2006; **28**(7):947–958.
12. Narasimhan S, Nagarajaiah S. A STFT semiactive controller for base isolated buildings with variable stiffness isolation systems. *Engineering Structures* 2004; **27**(4):514–523.
13. Alhan C, Gavin HP, Aldemir U. Optimal control: basis for performance comparison of passive and semiactive isolation systems. *Journal of Engineering Mechanics* 2006; **132**(7):705–713.
14. Ali SF, Ramaswamy A. Hybrid structural control using magnetorheological dampers for base isolated structures. *Smart Materials and Structures* 2009; **18** 055011, 1–16.
15. Shook DA, Roschke PN, Ozbulut OE. Superelastic semi-active damping of a base-isolated structure. *Structural Control and Health Monitoring* 2008; **15**(5):746–768.
16. Calabrese A, Spizzuoco M, Serino G, Della Corte G, Maddaloni G. Shake table investigation of a novel, low cost, base isolation technology using recycled rubber. *Structural Control and Health Monitoring* 2014. doi:10.1002/stc.1663.
17. Magliulo G, Petrone C, Capozzi V, Maddaloni G, Lopez P, Talamonti R, Manfredi G. Shake table tests on infill plasterboard partitions. *The Open Construction and Building Technology Journal* 2012; **6**(1):155–163.
18. Magliulo G, Petrone C, Capozzi V, Maddaloni G, Lopez P, Manfredi G. Seismic performance evaluation of plasterboard partitions via shake table tests. *Bulletin of Earthquake Engineering* 2013. doi:10.1007/s10518-013-9567-8.
19. Spizzuoco M, Calabrese A, Serino G. Innovative low-cost recycled rubber–fiber reinforced isolator: experimental tests and finite element analyses. *Engineering Structures* 2014; **76**:99–111.
20. Caterino N, Spizzuoco M, Occhiuzzi A. Understanding and modelling the physical behaviour of magnetorheological dampers for seismic structural control. *Smart Materials and Structures* 2011; **20**(6):065013, 1–19.
21. Caterino N, Spizzuoco M, Occhiuzzi A. Promptness and dissipative capacity of MR dampers: experimental investigations. *Structural Control and Health Monitoring* 2013; **20**(12):1424–1440.

22. NTC. Nuove norme tecniche per le costruzioni. DM 14 gennaio 2008, Gazzetta Ufficiale n. 29 del 4 febbraio 2008 – Supplemento Ordinario n. 30 (in Italian).
23. Iervolino I, Maddaloni G. Cosenza E Eurocode 8 compliant real record sets for seismic analysis of structures. *Journal of Earthquake Engineering* 2014; **12**(1):54–90.
24. Magliulo G, Maddaloni G, Petrone C. Comparison among different scaling methods for earthquake records used for seismic nonlinear analysis of structures. *Disaster Advances* 2014; **7**(1):39–49.
25. Occhiuzzi A. Additional viscous dampers for civil structures: analysis of design methods based on modal damping ratios. *Engineering Structures* 2009; **31**(5):1093–1101.
26. Moore BC. On the flexibility offered by state feedback in multivariable systems beyond closed loop eigenvalue assignment. *IEEE Transactions on Automatic Control* 1976; **AC-21**:689–692.

DOI: 10.1002/stc